LETTER

Chinese Journal of Structural Chemistry

Cyano and Isocyano-substituted Tetraphenylethylene with AIE Behavior and Mechanoresponsive Behavior

Qing Liu[1], Shusheng Yue[1], Zhangqiang Yan[1], Yongfa Xie[1]* and Hu Cai[1]*

[1]*School of Chemistry and Chemical Engineering, Nanchang University, Nanchang 330031, China*

ABSTRACT Dual-functional materials with AIE behavior and mechanoresponsive behavior have attracted considerable attention due to their promising applications in mechano-sensors, optical storage, solid-state optoelectric devices and bioimage systems. AIEgens bearing tetraphenylethylene (TPE) core become elementary building blocks in many fluorescent functional materials. In this article, cyano- and isocyano-electronic withdrawing groups are incorporated with TPE skeleton to form tetracyanophenylethylene (TPE-CN) and tetraisocyanophenylethylene (TPE-NC). Their structures are confirmed by NMR, Mass Spectra and single crystal X-ray measurement. These two isomers reflect aggregation-induced emission (AIE) property in solution state and mechanochromic behavior in solid state. Interestingly, their luminescent intensities, quantum yields and fluorescent lifetime in solid state have an obvious increase upon grinding. The theoretical calculation of these two compounds clarify their difference in optical properties. The mechanochromic mechanism is also intensively explained by powder X-ray measurements.

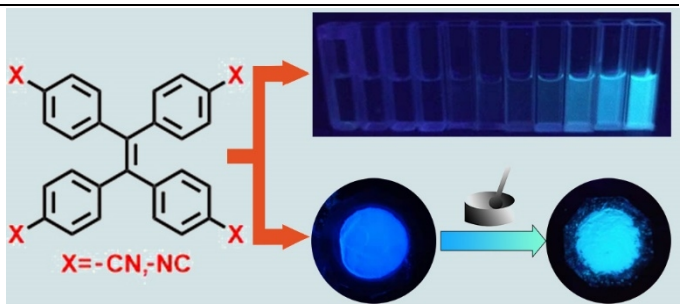

Keywords: cyano-group, isocyano-group, tetraphenylethlene (TPE), aggregation induced emission (AIE), mechanochromic

n INTRODUNTION

Aggregation induced emission (AIE) is a process which is in contrast to the notorious effect of aggregation-caused quenching (ACQ) process,[1] in which non-emissive molecules are induced to emit light by molecular aggregation. Since it was first discovered by Tang in 2001,[2] AIE phenomenon has arisen more and more attention due to its application in bioimage or bioprobe systems and solid-state optoelectronic devices.[3-9] Typical AIEgens bearing cores-tetraphenylethylene (TPE) have been intensively studied,[10-13] and become elementary building blocks in many fluorescent functional materials. In recent years, some new AIE building blocks have been continually explored, such as thiophene-triphenylamine (TTP),[14-17] tetraphenylpyrazine (TPP),[18-20] quinoline-malononitrile (QM),[21-23] 9,10-distrylanthracene (DSA),[24-26] benzothiadiazole (BT),[27-29] and quinoxaline,[30-33] and some fluorescent coordination molecules[34-36] based on TPE are also reported in recent years. However, single-functional materials with AIE behavior could not meet the requirements of rapid development of photoluminescent and electronic devices in modern society. Dual- or multi-functional materials are attracting more attention by researchers or engineers.[37] Though a few materials showing not only AIE but also mechanoresponsive behaviors have been reported recently[38-42], these dual-functional materials still need dig deeply since they are used to construct mechano-sensors[12,41,43-45] and applied in the field of anti-counterfeiting.[46,47] Accordingly, exploring multi-functional AIE-active fluorescent materials is of critical significance for promoting the development of imaging technology and meeting the requirements of electronic devices. Among the vast amount of tetraphenylethylene derivatives for AIE luminogens, some of them display mechanoresponsive property.[12,48,49] Here, we incorporate cyano-group (-CN) and isocyano-group (-NC) to the TPE skeleton to form two TPE derivatives (TPE-CN and TPE-NC) (Scheme 1), since these two groups with high conjugation with the benzene rings of TPE skeleton and their strong withdrawing property could result in the relative high stability and generally chemical unreactive. Owing to their unique electronic structures, aromatic nitrile compounds have been intensively used in dyes,[50-52] anti-cancer,[53] semiconductors,[54,55] and photocatalysis,[56-59] and aromatic isonitriles have been used as powerful photosensitizers,[60,61] mechano-response materials,[62] organic complexes,[63-65] etc. In this work, we synthesized the compound TPE-CN and its isomer TPE-NC. Both of these isomers (TPE-CN and TPE-NC) reveal AIE properties in the solution state and mechano-responsive properties in the solid state. The details are studied by fluorescent spectra in solution, and their change of photoluminescent properties by mechanical force in solid state reveal the mechanochromic behavior. Their mechanochromic mechanism was also studied by powder X-ray measurements.

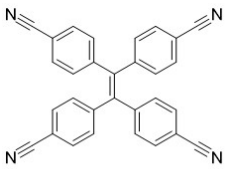

TPE-CN

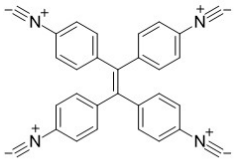

TPE-NC

Scheme 1. Molecular structures of TPE-CN and TPE-NC.

DOI: 10.14102/j.cnki.0254-5861.2021-0049

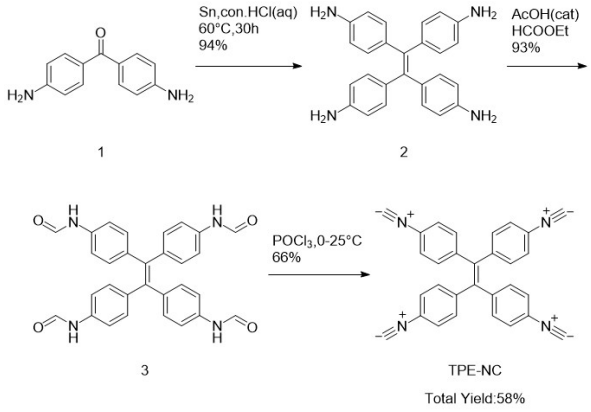

Scheme 2. Synthetic procedure of TPE-NC.

n RESULTS AND DISCUSSION

Synthesis of TPE-CN and TPE-NC. TPE-CN is a known molecule. It was synthesized according to the procedure in the literature.[66] Its excited behavior and electrochromic properties were studied in 1981[67] and 2019,[68] respectively, and it was also used as a unit to construct MOF functional materials.[69,70] Its isomer TPE-NC was synthesized from a commercially available compound **1** followed by 3 steps reactions: reaction of compound **1** with tin in concentrated hydrochloric acid obtains tetra(4-aminophenyl)ethene **2**, and a followed formylation of compound **2** with ethyl formate gives formamide **3**, and then a dehydration of compound **3** by phosphorus oxychloride in the presence of triethylamine affords the target isomer TPE-NC (Scheme 2). This molecule was also reported by W. Shi and was used as monomer to form polymer for catalyst field.[71] However, their fluorescent properties in solution and solid state have not been extensively studied.

AIE Characteristics. It is well known that TPE skeleton has been widely used for the construction of AIE-based functional materials.[10-13,72] Since both tetra(4-cyanophenyl)ethylene and its isomer contain TPE unit, the subsequent work could focus on investigating their AIE behavior by photoluminescent spectra at room temperature. All the fluorescent measurements were carried out in the mixed solution of THF/H_2O with different volume fractions of water (f_w). Water and THF were used because these two isomers are soluble in THF but insoluble in water. The existing forms of the two isomers would change from the dilute solution state in pure THF to the aggregated state in the mixed solvents by increasing the water fraction. Firstly, we prepared the dilute solution of these two isomers in mixed solvents with increasing the water fraction and excited with handle UV-visible light (365 nm), then their fluorescent brightness increased (Figure 1a, b). Secondly, the emission spectra were measured, and the AIE phenomenon is proved by the spectra of the solution of the isomers in mixed solvents with different water fraction. In dilute THF solution of these two isomers with the water fraction lower than 80%, almost no fluorescence is observed. When the fraction (f_w) of water is less than 92%, very low emission intensity is observed for these two isomers, and the emission peaks of TPE-CN and TPE-NC appear at 483 and 492 nm, respectively. However, the emission

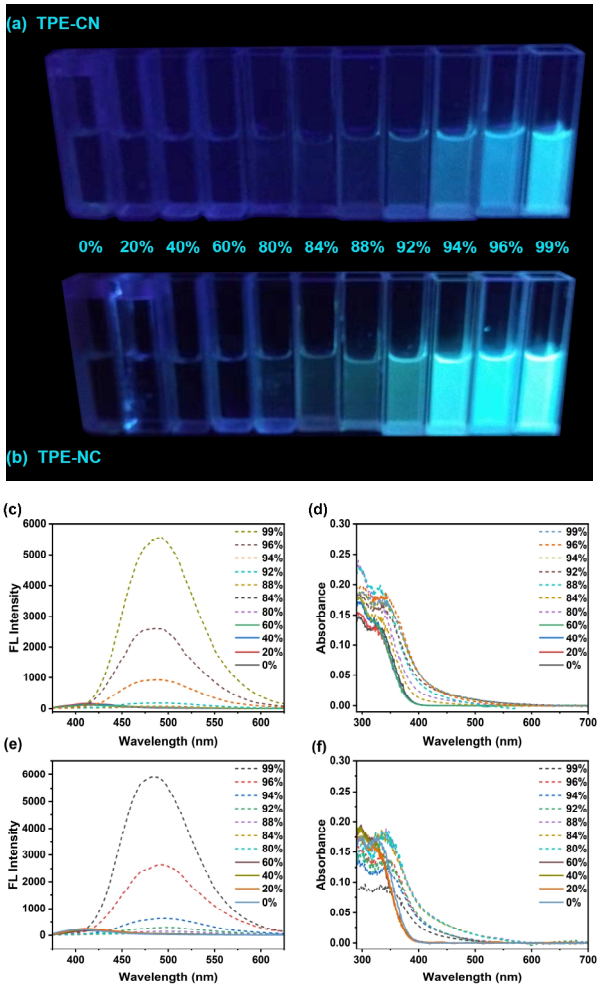

Figure 1. Photoluminescent image of TPE-CN (a) and TPE-NC (b) with different water diffraction in THF (1.0×10^{-5} mol L^{-1}) under handle UV-visible light (365 nm). The photoluminescent spectra of diluted solution (1.0×10^{-5} mol L^{-1}) of TPE-NC (c) and TPE-CN (e) in THF-water mixture with different water content (0%–99%) (excited with 340 and 320 nm, respectively). UV-visible absorption spectra of TPE-CN (d) and TPE-NC (f) in THF-water mixture with different water content (0%–99%).

intensity dramatically increase for the two isomers when the water fraction is up to 99% (Figure 1c, d). UV-visible absorption measurements for TPE-CN and TPE-NC in H_2O/THF mixtures with different water contents were also carried out. The spectra tails in the long wavelength region in H_2O/THF mixtures with water contents higher than 80% are caused by the light-scattering effect. These phenomena imply that the isomers formed nanoparticles in H_2O/THF mixtures with water contents higher than 80% (Figure 1d, f). Consequently, the AIE phenomenon could be explained as follows: the very high water fraction in the mixed solution resulted in the aggregation of TPE-CN and TPE-NC molecules, thus restricting the intramolecular rotation and intermolecular interaction and then leading to a higher emission energy. The AIE phenomena for these two isomers also represent in other solvents for such as CH_3CN, DMF, and DMSO (Figure S1–S4). With improv-

DOI: 10.14102/j.cnki.0254-5861.2021-0049

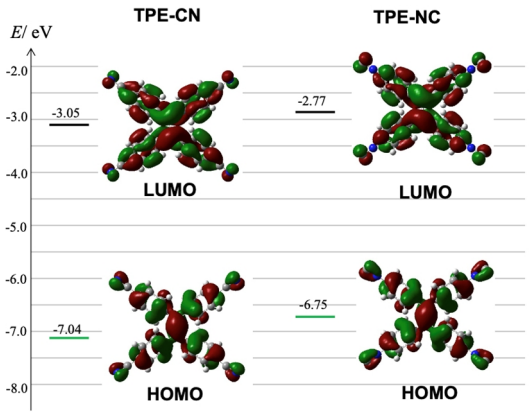

Figure 2. DFT calculations of frontier orbitals of TPE-NC and TPE-CN at PBE0/def2-SVP level.

ing the polarity of the solvents, their emission intensities increase. Other TPE derivatives with similar properties were also described by Chen *et al* (Figure S5).[73]

In order to uncover the influence of geometric and electronic structures of TPE-CN and TPE-NC on their optical properties, the density functional theory (DFT) calculations for these two compounds were performed by Gaussian 09 W program at the PBE0/def2-SVP level after optimization of these two isomers. The energy levels diagram and spatial distribution of the frontier orbitals (HOMO and LUMO) for TPE-CN and TPE-NC are shown in Figure 2. The overall electron density of LUMOs of these two molecules is almost distributed in the whole molecules, while the LUMO of TPE-NC has a nodal position on the nitrogen atom. The LUMO energy levels are –3.05 and –2.77 eV for TPE-CN and TPE-NC, respectively. The overall electron density of HOMO for TPE-CN and TPE-NC is also delocalized in the whole molecule. They also have small difference in HOMO energy levels of –7.04 and –6.75 eV for TPE-CN and TPE-NC, respectively. The small difference of energy levels and electron distribution of LUMO orbitals of these two molecules is probably attributed to the cyano-group which has higher electron-withdrawing ability than the isocyano-group.

The dilute solution of TPE-CN in THF shows two absorption bands (around 296 and 327 nm), and the dilute solution of TPE-NC in THF shows two absorption bands (around 298 and 327 nm) (Figure S6). Their two absorption bands were confirmed by the TD-DFT calculated data (Figure S7) even though there are tens of nanometers difference. The higher absorption band (327 nm) of TPE-CN is mainly contributed by the transition (3.30 eV) from HOMO to LUMO with an oscillator strength of 0.60, while its lower absorption band (296 nm) is mainly contributed by the transition (4.01 eV) from HOMO to LUMO+1 with an oscillator strength of 0.48 (Figure S8 and Table S1). The higher absorption band (327 nm) of TPE-NC is mainly contributed by the transition (3.28 eV) from HOMO to LUMO with an oscillator strength of 0.63, while its lower absorption band (298 nm) is mainly contributed by the transition (4.00 eV) from HOMO to LUMO+1 with an oscillator strength of 0.51 (Figure S8 and Table S1). According to the above calculated excitation energies and molecular orbitals of excited states after optimizing the molecules, they have two similar absorption bands in THF solution since the transitions contributing to the absorption bands have similar energy differences and the molecular orbitals for the transitions have similar orbital distribution.

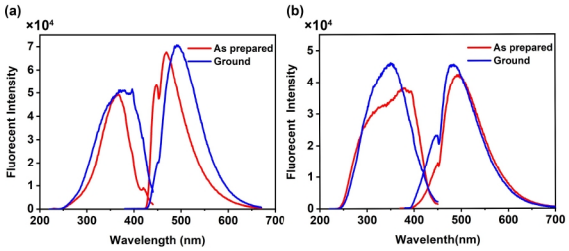

Figure 3. Excitation and emission spectra of TPE-CN (a) and TPE-NC (b): the left and right parts in each figure present excitation and emission spectra in the solid state, respectively. As prepared samples (red line), ground samples (blue line).

Mechanochromic Characteristics. TPE-CN and TPE-NC should adopt twisted spatial conformations due to the spatial hinderance between neighbored phenyl rings in these two isomers (Dihedral angles of these two isomers in the optimized lowest energy state and in crystal state can be found in Figure S9–12). The specially twisted conformation of TPE-CN and TPE-NC disfavors close molecular packing and π-π interactions in the solid state, which may enable the two isomers to have solid state emission and MFC behavior.[38] Then the optical properties of TPE-CN and TPE-NC in solid state were investigated before and after grinding. As presented in Figure 3, the as-synthesized sample of TPE-CN shows a maximum emission shift from 468 to 493 nm before and after grinding. Its shoulder emission peak manifests an obvious change before (447 nm) and after grinding (450 nm). Correspondingly, a change from blue fluorescence to light blue fluorescence is found in the solid state (Figure 4a). However, reversible fluorescence phenomenon is not displayed after fuming by several solvents (THF, CH_3CN, and CH_2Cl_2) or heating (Figure 4a). The maximum excitation peak of solid-state TPE-CN also revealed a red-shift from 365 to 380 nm before and after grinding (Figure 3a). For the isocyano-substituted analogue TPE-NC, the as-synthesized sample also showed a max emission peak at 482 nm and a shoulder emission peak at 447 nm in the solid state. After grinding by a pestle and mortar, the max fluorescence peak shifted to 493 nm, and the shoulder fluorescence peak nearly disappears, corresponding with a blue fluorescence to light blue fluorescence (Figure 4b). Reversible fluorescence phenomenon for TPE-NC is not

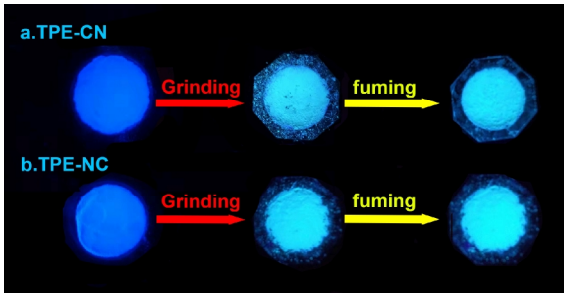

Figure 4. (a) The pristine sample of TPE-CN after grinding and fuming with THF. (b) The pristine sample of TPE-NC after grinding and fuming with THF.

DOI: 10.14102/j.cnki.0254-5861.2021-0049

Table 1. Maximum Excitation and Emission Peaks, Lifetime and Quantum Yield of TPE-CN and TPE-NC in Solid State

	Excitation	Emission	Life time	Quantum yield
TPE-CN As-synthesized	365 nm	468 nm	2.32 ns	4.7%
TPE-CN ground	380 nm	493 nm	3.96 ns	36.0%
TPE-NC As-synthesized	347 nm	482 nm	1.95 ns	28.6%
TPE-NC ground	373 nm	493 nm	3.98 ns	40.4%

found, either (Figure 4b). The maximum excitation peak of solid-state TPE-NC shows a red shift from 347 to 373 nm (Figure 3b).

The variable optical properties of these two isomers are probably owing to the crystallinity change before and after grinding in the solid state. Foreseeingly, their fluorescent lifetime and quantum yield should be changed by grinding in the solid state. The fluorescent lifetime of luminogen TPE-CN increases from 2.32 nm to 3.96 ns (Table 1 and Figure S14–15), and the quantum yield dramatic increases from 4.7% to 36.0% by grinding. The dramatic enhancement of the quantum yield probably is attributed to the molecular arrangement and the dihedron angles of the neighboring benzene rings in TPE skeleton changed by grinding as illustrated by the PXRD below. For the cyano analogue TPE-NC, it also shows an increase of fluorescent lifetime from 1.95 to 3.98 ns (Figure S16–17) and an increase of fluorescent quantum yield from 28.6% to 40.4% (Table 1). This enhancement of emission efficiency after grinding is in contrast to a TPE derivative (TPEOSi) with cyano-groups reported previously[74] and the azine luminogen which exhibits strong emission both in crystalline and powder state.[75]

To uncover the mechanism of this mechanochromic phenomenon, we carried out powder X-ray diffraction (PXRD) characteristics for the samples of TPE-CN and TPE-NC in solid state before and after grinding as well as by fuming. As shown in Figure 5, before grinding, these samples show strong and sharp diffraction peaks for TPE-CN and TPE-NC, indicating that the aggregate is well ordered in the crystalline state. After grinding, the intensity of the diffraction peaks is weakened (Figure 5a) and some peaks cannot be found (Figure 5b: peaks at 15° and 25° disappear after grinding), indicating that the initial ordered arrangement of the crystals is changed by grinding. After fuming the ground samples of these two isomers, the intensity of the PXRD decreases dramatically, implying that they become much more amorphous after

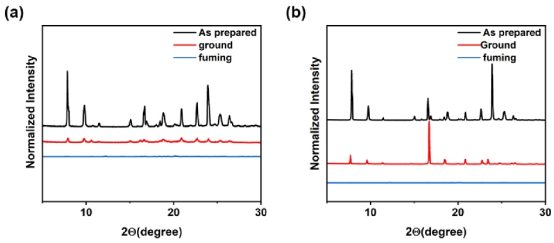

Figure 5. PXRD curve for TPE-CN (a) and TPE-NC (b) before and after grinding, and fuming with THF.

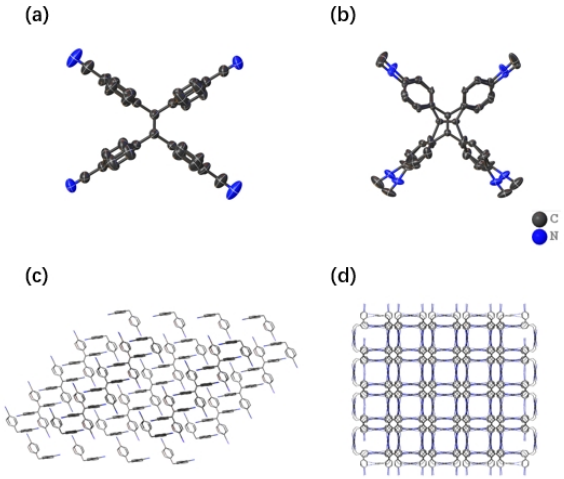

Figure 6. Crystal structure of TPE-CN (a) and TPE-NC (b), water molecules in the crystal lattice are masked in the CIF data. Crystal packing structure of TPE-CN (c) and TPE-NC (d).

fuming by the THF solvent.

Crystal Structure. Colorless crystals of TPE-CN suitable for XRD were obtained by cooling the hot saturated solution of tetra(4-cyanophenyl)ethylene in ethanol. The crystal structure and cell parameters were determined by single-crystal X-ray diffraction with Mo*Ka* radiation, as shown in Figure 6a. This compound crystallizes in symmetric monoclinic space group *C*2/*c*, with its asymmetric unit containing half of the molecule. It adopts a highly twisted structure (four benzene rings are not in a plane), and the neighbored phenyl rings have dihedral angles of 70.2° (Figure S10). Since the benzene ring can rotate along the C–C bond, two phenyl rings in its crystal structure present positional disordered states with proportions of 38% and 62%. In the molecular stacking diagram, we can find intermolecular p-p stacking of the neighbored phenyl rings with a distance of 3.9 Å (Figure S13).

For the crystal of TPE-NC, its asymmetric unit also contains a half of the molecule. It crystallizes in a space group of $I4_1/acd$. In the crystal, one molecule presents two disordered states with proportions of 75% and 25%. In one part of the molecule, the neighbored phenyl rings have dihedral angles of 63.8°, 69.3°, 69.3° and 88.4° (Figure S11), while in the other part, neighboring phenyl rings have dihedral angles of 58.0°, 73.1°, 80.1° and 80.1° (Figure S12). Along the *c*-axis, it forms a highly neat hole-like structure (Figure 6d).

n CONCLUSION

In conclusion, two isomers based on TPE (TPE-CN and TPE-NC) were synthesized and their structures were characterized by EI-MS, NMR, and crystal structure. Both of them show a practical AIE phenomenon in the THF/water solution system. They also reveal mechanochromic emission change in the solid state by grinding, and the fluorescent quantum yield and lifetime increase upon grinding. Their optical properties in solution and solid states were also confirmed by the DFT and TD-DFT calculations. TPE-CN and TPE-NC with AIE and mechanoresponsive behaviors may have

DOI: 10.14102/j.cnki.0254-5861.2021-0049

potential application in fluorescent sensor and mechano-sensor materials.

n EXPERIMENTAL

Materials and Methods. All commercially available chemicals and regents were used without further purification. NMR spectra were recorded on Agilent Technologies 400 MHz spectrometers. Chemical shifts are reported in parts per million (ppm) down field from TMS with the solvent resonance as the internal standard. Coupling constants (J) are reported in Hz and referred to apparent peak multiplications. High-resolution MS was obtained using an Agilent Q-TOF 6545 instrument equipped with ESI source. The UV-visible absorption spectra were measured on a Perkin Elmer Lambda 35 UV-visible spectrophotometer. The emission and excitation spectra together with the emission lifetime in solid states were determined on an Edinburgh analytical instrument (FLS920 fluorescence spectrometer). Powder XRD patterns were determined by a BRUKER-axs D8-Andvance X-ray diffractometer and using Cu*Kα* radiation (*λ* = 0.15406 nm, 40 kV and 30 mA). Measurement angles range from 5° to 50° at a step of 0.02°. Single-crystal XRD was measured using a Rigaku Saturn 724+ CCD diffractometer with Mo*Kα* radiation (*λ* = 0.71073 Å). Data collection, cell refinement, and data reduction were performed using Rigaku Crystal Clear software package. The structures were solved by direct methods and refined by the full-matrix least-squares method based on F^2 by means of the SHELXLTL software package. All non-H atoms were refined anisotropically. All H atoms were generated geometrically and refined using a “riding” model.

Synthesis of 1,1',2,2'-Tetra(4-aminophenyl)ethylene. The procedure was adapted from literature[76] with some modification. 4,4'-Diaminobenzophenone (6.0 g, 28.3 mmol) was dissolved in 300 mL of concentrated HCl aqueous solution. The mixture was stirred at 60 °C for 20 min, followed by slowly adding Sn (25 g, powder). The reaction mixture was heated to 75 °C for 30 h. The resulted suspension was diluted with water, giving a transparent yellow solution. The pH of the mixture was adjusted to 14 by slow addition of NaOH solid. The mixture was filtered and washed with water. The filter cake was washed with a mixture of DCM (200 mL) and ethanol (50 mL) for 5 times. The obtained filtrate was washed with water and extracted with DCM (150 mL×3). The organic layers were combined and dried over Na_2SO_4. After evaporation of the organic solvents in vacuum, a yellow solid (5.23 g, yield: 94%) was obtained. This crude material was used for next step without further purification. Its NMR data are identical with the value[77] reported by Wang. TLC R_f = 0.31 (methanol/dichloromethane = 1:35) ^{1}H NMR (400 MHz, DMSO-d_6) δ 6.58 (d, J = 8.0 Hz, 8H), 6.27 (d, J = 8.2 Hz, 8H), 4.85 (s, 8H).^{13}C NMR (101 MHz, DMSO-d_6) δ 146.12, 136.71, 133.02, 131.78, 113.24.

Synthesis of 1,1',2,2'-Tetra(4-formamidophenyl)ethylene. To a one-neck round flask were added 1,1',2,2'-tetra(4-aminophenyl)ethylene (5.23 g, 13.3 mmol), ethyl formate (80 mL) and acetic acid (2.6 mL). The mixture was refluxed overnight. TLC indicated that the starting material was consumed. The reaction mixture was cooled and filtered. The filtercake was washed with ethyl formate (20 mL×4). The collected solid was dried, affording a pale solid (6.25 g, 12.3 mmol, yield: 93%). The purity of this compound was checked by TLC (R_f = 0.26 (methanol/dichloromethane = 1/8, 254, 365 nm: green fluorescence) analysis, and the crude material was used for the next step without further purification.

Synthesis of 1,1',2,2'-Tetra(4-isocyanophenyl)ethylene. 1,1', 2,2'-Tetra(4-formamidophenyl)ethylene (6.25 g, 12.3 mmol) was added in 115 mL of dry CH_2Cl_2 (dried by CaH_2 prior to use) under N_2 atmosphere. The mixture was cooled to –5 °C, and anhydrous triethylamine (21.7 mL, 156.2 mmol) was added slowly via a syringe. While keeping the temperature at –10 to –5 °C, phosphorus oxychloride (4.7 mL, 50.8 mmol) was slowly added via a syringe within 30 min. The reaction mixture was stirred at –10 to 25 °C and stirred for about 1 h. The resulting brown solution was cooled to –10 °C, and aqueous K_2CO_3 (10.5 g in 100 mL water) was slowly added within 30 min. The organic phase was separated, and the aqueous phase was extracted with ethyl acetate (100 mL). The obtained organic phases were combined, dried over Na_2SO_4, filtered and concentrated. Purification of the residue was accomplished by flash column chromatography on silica gel (ethyl acetate (EA)/petroleum ether (PE) = 1/4), affording a colorless solid (3.55 g, yield: 66%). TLC R_f = 0.29 (EA/PE = 1/4). 1H NMR (400 MHz, chloroform-d) δ 7.17 (d, J = 8.2 Hz, 8H), 6.99 (d, J = 8.0 Hz, 8H). 13C NMR (101 MHz, chloroform-d) δ 165.54, 142.90, 140.62, 132.16, 126.61, 125.82. HRMS (ESI, m/z) $[M+H]^+$ calcd. for $C_{30}H_{17}N_4$: 433.1448; found: 433.1450.

n ACKNOWLEDGEMENTS

This work is supported by the National Natural Science Foundation of China (21905127, 22065023, 21861026, 22075123) and Natural Science Foundation of Jiangxi Province (20212BAB203029). The authors also thank Associate Prof. Zhiyong Wang (Renmin University of China) for his DFT and TD-DFT theory calculation.

n AUTHOR INFORMATION

Corresponding authors. Emails: xieyf@ncu.edu.cn (Yongfa Xie) and caihu@ncu.edu.cn (Hu Cai)

n COMPETING INTERESTS

The authors declare no competing interests.

n ADDITIONAL INFORMATION

The crystal structures (TPE-CN and TPE-NC) can be downloaded from the Cambridge Crystal Database (CCDC No. 2112910 and 2112911). DFT and TD-DFT calculations, dihedral angles, and NMR data are in the Supplementary Information available at http://manu30.magtech.com.cn/jghx/EN/10.14102/j.cnki.0254-5861.2021-0049

For submission: https://mc03.manuscriptcentral.com/cjsc

n REFERENCES

(1) Birks, J. B. *Photophysics of Aromatic Molecules* (Wiley Monographs in Chemical Physics): Wiley-Interscience **1970**.

(2) Luo, J. D.; Xie, Z. L.; Lam, J. W. Y.; Cheng, L.; Chen, H. Y.; Qiu, C. F.; Kwok, H. S.; Zhan, X. W.; Liu, Y. Q.; Zhu, D. B.; Tang, B. Z. Aggregation-induced emission of 1-methyl-1,2,3,4,5-pentaphenylsilole. *Chem. Commun.* **2001**, 18, 1740–1741.

DOI: 10.14102/j.cnki.0254-5861.2021-0049

(3) Khan, I. M.; Niazi, S.; Iqbal Khan, M. K.; Pasha, I.; Mohsin, A.; Haider, J.; Iqbal, M. W.; Rehman, A.; Yue, L.; Wang, Z. Recent advances and perspectives of aggregation-induced emission as an emerging platform for detection and bioimaging. *Trac-Trends Anal. Chem.* **2019**, 119, 115637.
(4) Zhang, Z.; Chen, D. D.; Liu, Z. H.; Wang, D.; Guo, J. T.; Zheng, J.; Qin, W. P.; Wu, C. F. Near-infrared polymer dots with aggregation-induced emission for tumor imaging. *ACS Appl. Polym. Mater.* **2020**, 2, 74–79.
(5) Kwok, R. T. K.; Leung, C. W. T.; Lam, J. W. Y.; Tang, B. Z. Biosensing by luminogens with aggregation-induced emission characteristics. *Chem. Soc. Rev.* **2015**, 44, 4228–4238.
(6) Zhao, D. Y.; Fan, F.; Cheng, J.; Zhang, Y. L.; Wong, K. S.; Chigrinov, V. G.; Kwok, H. S.; Guo, L.; Tang, B. Z. Light-emitting liquid crystal displays based on an aggregation-induced emission luminogen. *Adv. Opt. Mater.* **2015**, 3, 199–202.
(7) Mei, J.; Leung, N. L. C.; Kwok, R. T. K.; Lam, J. W. Y.; Tang, B. Z. Aggregation-induced emission: together we shine, united we soar! *Chem. Rev.* **2015**, 115, 11718–11940.
(8) Zhan, C.; You, X.; Zhang, G. X.; Zhang, D. Q. Bio-/chemosensors and imaging with aggregation-induced emission luminogens. *Chem. Rec.* **2016**, 16, 2142–2160.
(9) Mei, J.; Huang, Y. H.; Tian, H. Progress and trends in AIE-based bioprobes: a brief overview. *ACS Appl. Mater. Interfaces* **2018**, 10, 12217–12261.
(10) La, D. D.; Bhosale, S. V.; Jones, L. A.; Bhosale, S. V. Tetraphenylethylene-based AIE-active probes for sensing applications. *ACS Appl. Mater. Interfaces* **2018**, 10, 12189–12216.
(11) Jiang, B.; Zhang, C. W.; Shi, X. L.; Yang, H. B. AIE-active metal-organic coordination complexes based on tetraphenylethylene unit and their applications. *Chin. J. Polym. Sci.* **2019**, 37, 372–382.
(12) Yang, Z. Y.; Chi, Z. H.; Mao, Z.; Zhang, Y.; Liu, S. W.; Zhao, J.; Aldred, M. P.; Chi, Z. G. Recent advances in mechano-responsive luminescence of tetraphenylethylene derivatives with aggregation-induced emission properties. *Mater. Chem. Front.* **2018**, 2, 861–890.
(13) Zhao, Z. J.; Lam, J. W. Y.; Tang, B. Z. Tetraphenylethene: a versatile AIE building block for the construction of efficient luminescent materials for organic light-emitting diodes. *J. Mater. Chem.* **2012**, 22, 23726–23740.
(14) Wang, D.; Su, H. F.; Kwok, R. T. K.; Hu, X. L.; Zou, H.; Luo, Q. X.; Lee, M. M. S.; Xu, W. H.; Lam, J. W. Y.; Tang, B. Z. Rational design of a water-soluble NIR AIEgen, and its application in ultrafast wash-free cellular imaging and photodynamic cancer cell ablation. *Chem. Sci.* **2018**, 9, 3685–3693.
(15) Xu, W. H.; Lee, M. M. S.; Zhang, Z. H.; Sung, H. H. Y.; Williams, I. D.; Kwok, R. T. K.; Lam, J. W. Y.; Wang, D.; Tang, B. Z. Facile synthesis of AIEgens with wide color tunability for cellular imaging and therapy. *Chem. Sci.* **2019**, 10, 3494–3501.
(16) Zhang, J. J.; Chen, Q.; Fan, Y. Q.; Qiu, H. Y.; Ni, Z. G.; Li, Y.; Yin, S. C. Near-infrared-emitting difluoroboron β-diketonate dye with AIE characteristics for cellular imaging. *Dyes Pigment.* **2021**, 193, 109500.
(17) Gao, Y. T.; Zhang, H.; Jiang, T.; Yang, J.; Li, B.; Li, Z.; Hua, J. L. Synthesis, two-photon absorption and AIE properties of multibranched thiophene-based triphenylamine derivatives with triazine core. *Sci. China: Chem.* **2013**, 56, 1204–1212.
(18) Chen, M.; Li, L. Z.; Nie, H.; Tong, J. Q.; Yan, L. L.; Xu, B.; Sun, J. Z.; Tian, W. J.; Zhao, Z. J.; Qin, A. J.; Tang, B. Z. Tetraphenylpyrazine-based AIEgens: facile preparation and tunable light emission. *Chem. Sci.* **2015**, 6, 1932–1937.
(19) Pan, L. X.; Wu, H. Z.; Liu, J. K.; Xue, K. Q.; Luo, W. W.; Chen, P.; Wang, Z. M.; Qin, A. J.; Tang, B. Z. Tetraphenylpyrazine based AIE luminogens: unique excited state decay and its application in deep-blue light-emitting diodes. *Adv. Opt. Mater.* **2019**, 7, 1801673.
(20) Guo, J. L.; Pan, L. X.; Song, B.; Gu, J. B.; Zeng, J. J.; Xu, X. T.; Wu, H. Z.; Zhao, Z. J.; Wang, Z. M.; Qin, A. J.; Tang, B. Z. Tetraphenylpyrazine decorated 1,3-di(9H-carbazol-9-yl)benzene (mCP): a new AIE-active host with enhanced performance in organic light-emitting diodes. *J. Mater. Chem. C* **2019**, 7, 11160–11166.
(21) Guo, Z. Q.; Shao, A. D.; Zhu, W. H. Long wavelength AIEgen of quinoline-malononitrile. *J. Mater. Chem. C* **2016**, 4, 2640–2646.
(22) Xia, Z. Q.; Shao, A. D.; Li, Q.; Zhu, S. Q.; Zhu, W. H. Substituent effect on quinoline-malononitrile AIE fluorescent properties. *Acta Chim. Sinica* **2016**, 74, 351–355.
(23) Guo, Z. Q.; Yan, C. X.; Zhu, W. H. High-performance quinoline-malononitrile core as a building block for the diversity-oriented synthesis of AIEgens. *Angew. Chem., Int. Ed.* **2020**, 59, 9812–9825.
(24) Zhang, X. Q.; Chi, Z. G.; Xu, B. J.; Jiang, L.; Zhou, X.; Zhang, Y.; Liu, S. W.; Xu, J. R. Multifunctional organic fluorescent materials derived from 9,10-distyrylanthracene with alkoxyl endgroups of various lengths. *Chem. Commun.* **2012**, 48, 10895–10897.
(25) He, J. T.; Xu, B.; Chen, F. P.; Xia, H. J.; Li, K. P.; Ye, L.; Tian, W. J. Aggregation-induced emission in the crystals of 9,10-distyrylanthracene derivatives: the essential role of restricted intramolecular torsion. *J. Phys. Chem. C* **2009**, 113, 9892–9899.
(26) Xu, B.; Tian, W. J. Aggregation induced emission of 9,10-distrylanthracene derivatives: molecular design and applications. *ACS Symp. Ser.* **2016**, 1226, 113–136.
(27) Liu, S. J.; Chen, C.; Li, Y. Y.; Zhang, H. K.; Liu, J. K.; Wang, R.; Wong, S. T. H.; Lam, J. W. Y.; Ding, D.; Tang, B. Z. Constitutional isomerization enables bright NIR-II AIEgen for brain-inflammation imaging. *Adv. Funct. Mater.* **2020**, 30, 1908125.
(28) Chen, S. H.; Qin, Z. H.; Liu, T. F.; Wu, X. Z.; Li, Y. J.; Liu, H. B.; Song, Y. L.; Li, Y. L. Aggregation-induced emission on benzothiadiazole dyads with large third-order optical nonlinearity. *Phys. Chem. Chem. Phys.* **2013**, 15, 12660–12666.
(29) Huo, J. N.; Zheng, Y. N.; Zhang, D.; Xu, H. X.; Li, Y. B.; Miao, Y. Q.; Shi, H. P.; Tang, B. Z. A rational design strategy for red thermally activated delay fluorescence emitter employing 2,1,3-benzothiadiazole skeleton with asymmetric structure. *Dyes Pigment.* **2021**, 196, 109781.
(30) Merkt, F. K.; Mueller, T. J. J. Synthesis and electronic properties of expanded 5-(hetero)aryl-thien-2-yl substituted 3-ethynyl quinoxalines with AIE characteristics. *Sci. China: Chem.* **2018**, 61, 909–924.
(31) Wang, B. B.; Liu, L.; Zhang, Y. Y.; Shen, L. J.; Wang, L. J.; Chen, A. b.; Feng, H. B.; Xiao, X. W. Novel diaryquioxaline derivatives with aggregation-induced emission characteristics for turn-on detection of Hg^{2+}. *Chin. Chem. Bull.* **2018**, 81, 525–530.
(32) Nirmalananthan, N.; Behnke, T.; Hoffmann, K.; Kage, D.; Gers-Panther, C. F.; Frank, W.; Mueller, T. J. J.; Resch-Genger, U. Crystallization and aggregation-induced emission in a series of pyrrolidinylvinylquinoxaline derivatives. *J. Phys. Chem. C* **2018**, 122, 11119–11127.
(33) Xiao, X. L.; Li, F. F.; Xiao, X. W.; Wen, Y. H. Synthesis, structure and aggregation-induced emission characteristics of two diarylquinoxaline derivatives. *Chin. J. Struct. Chem.* **2019**, 38, 1200–1206.
(34) Chen, M.; Wang, X. M.; He, Y. H.; Yang, J.; Wang, S.; Tong, B. H. Blue-green phosphorescent iridium complex with terdentate ligand. *Chin.*

DOI: 10.14102/j.cnki.0254-5861.2021-0049

J. Struct. Chem. **2016**, 35, 114–118.

(35) Liang, Y.; Xu, X. D.; Ni, J. L.; Li, J. F.; Wang, F. M. Synthesis, structure and fluorescence property of new Cd-MOFs based on a tetraphenylethylene (TPE) ligand. *Chin. J. Struct. Chem.* **2021**, 40, 193–198.

(36) Li, J. F.; Xu, X. D.; Lei, Z.; Wang, F. M. Synthesis, structure and fluorescence property of a new Mn-MOFs based on a tetraphenylethane (TPE) ligand. *Chin. J. Struct. Chem.* **2019**, 38, 797–802.

(37) Wang, C. P.; Kashi, C.; Ye, X. L.; Li, W. H.; Wang, G. E.; Xu, G. A zinc based coordination polymer: multi-functional material for humidity sensor and fluorescence applications. *Chin. J. Struct. Chem.* **2021**, 40, 1138–1144.

(38) Wang, Y.; Cheng, D. D.; Zhou, H. K.; Liu, J. R.; Liu, X. L.; Wang, Y. H.; Han, A. X.; Zhang, C. Tetraphenylethene-containing cruciform luminophores with aggregation-induced emission and mechanoresponsive behavior. *Dyes Pigment.* **2019**, 170, 107606.

(39) Peng, Y. X.; Liu, H. Q.; Shi, R. G.; Feng, F. D.; Hu, B.; Huang, W. Tetraphenyethylene-fused coumarin compound showing highly switchable solid-state luminescence. *J. Phys. Chem. C* **2019**, 123, 6197–6204.

(40) Hu, H.; Chen, Z.; Pu, S. Z. Fluorene-based aggregation-induced emission (AIE)-active tetraphenylethene derivatives: the effect of alkyl chain length on mechanofluorochromic behaviors. *Tetrahedron Lett.* **2021**, 67, 152846.

(41) Zhang, Z.; Cao, M. K.; Zhang, L.; Qiu, Z. J.; Zhao, W. J.; Chen, G.; Chen, X.; Tang, B. Z. Dynamic visible monitoring of heterogeneous local strain response through an organic mechanoresponsive AIE luminogen. *ACS Appl. Mater. Interfaces* **2020**, 12, 22129–22136.

(42) Kang, J. J.; Ni, J.; Li, Y. Q. Synthesis/crystal structure and luminescent mechanochromism of a square-planar Pt(II) complex based on 1,10-phenanthroline derivative. *Chin. J. Struct. Chem.* **2020**, 39, 140–146.

(43) Yu, T.; Ou, D. P.; Yang, Z. Y.; Huang, Q. Y.; Mao, Z.; Chen, J. R.; Zhang, Y.; Liu, S. W.; Xu, J. R.; Bryce, M. R.; Chi, Z. G. The HOF structures of nitrotetraphenylethene derivatives provide new insights into the nature of AIE and a way to design mechanoluminescent materials. *Chem. Sci.* **2017**, 8, 1163–1168.

(44) Zhang, F.; Zhang, R.; Liang, X. Z.; Guo, K. P.; Han, Z. X.; Lu, X. Q.; Xie, J. J.; Li, J.; Li, D.; Tian, X. 1,3-Indanedione functionalized fluorene luminophores: negative solvatochromism, nanostructure-morphology determined AIE and mechanoresponsive luminescence turn-on. *Dyes Pigment.* **2018**, 155, 225–232.

(45) Zheng, X. Y.; Bai, B. L.; Li, Z. M.; Wei, J.; Wang, H. T.; Li, M.; Xin, H. A fluorescent sensor for detection of grinding force and fluoride ion based on acylhydrazone derivative. *Dyes Pigment.* **2020**, 175, 108153.

(46) Chen, G. J.; Hong, W. Mechanochromism of structural-colored materials. *Adv. Opt. Mater.* **2020**, 8, 2000984.

(47) Huang, G. X.; Xia, Q.; Huang, W. B.; Tian, J. W.; He, Z. K.; Li, B. S.; Tang, B. Z. Multiple anti-counterfeiting guarantees from a simple tetraphenylethylene derivative – high-contrasted and multi-state mechanochromism and photochromism. *Angew. Chem., Int. Ed.* **2019**, 58, 17814–17819.

(48) Chi, Z. G.; Zhang, X. Q.; Xu, B. J.; Zhou, X.; Ma, C. P.; Zhang, Y.; Liu, S. W.; Xu, J. R. Recent advances in organic mechanofluorochromic materials. *Chem. Soc. Rev.* **2012**, 41, 3878–3896.

(49) Yang, Z. Y.; Mao, Z.; Yu, T.; Zhang, Y.; Liu, S. W.; Xu, J. R.; Chi, Z. G. Mechano-responsive AIE luminogens. *ACS Symp. Ser.* **2016**, 1226, 221–259.

(50) Astbury, C.; Conway, L. K.; Gillespie, C.; Hodge, K.; Innes, E.; Kennedy, A. R. A structural study of seven salt forms of sulfonated azo dyes containing nitrile functional groups. *Dyes Pigment.* **2013**, 97, 100–104.

(51) An, M.; Sarker, A. K.; Jung, D. C.; Hong, J. D. An organic nitrile dye with strong donor and acceptor groups for dye-sensitized solar cells. *Bull. Korean Chem. Soc.* **2011**, 32, 2083–2086.

(52) Wen, W.; Yu, J. S.; Li, L.; Ma, T.; Jiang, Y. D. Spectral characteristics of white organic light-emitting devices based on a novel nitrile fluorescence dye. *Spectrosc. Spect. Anal.* **2009**, 29, 589–592.

(53) Di, L. Synthesis, anti-lung cancer activity and docking study of new organic compounds. *Chin. J. Struct. Chem.* **2020**, 39, 1119–1125.

(54) Han, Y. S.; Kim, J. Y. Perovskite solar cell having N-type semiconductor modified with nitrile compound capable of improving the efficiency, and method for manufacturing same. KR2019097662, **2019**.

(55) Xiong, Y.; Qiao, X. L.; Li, H. X. Nitrile-substituted thienyl and phenyl units as building blocks for high performance n-type polymer semiconductors. *Polym. Chem.* **2015**, 6, 6579–6584.

(56) Lin, H. X.; Chen, C. P.; Zhou, T. H.; Zhang, J. Two-dimensional covalent-organic frameworks for photocatalysis: the critical roles of building block and linkage. *Sol. RRL.* **2021**, 5, 2000458.

(57) Jiang, X. H.; Zhang, L. S.; Liu, H. Y.; Wu, D. S.; Wu, F. Y.; Tian, L.; Liu, L. L.; Zou, J. P.; Luo, S. L.; Chen, B. B. Silver single atom in carbon nitride catalyst for highly efficient photocatalytic hydrogen evolution. *Angew. Chem., Int. Ed.* **2020**, 59, 23112–23116.

(58) Zhao, C. B.; Qiang, Z.; Jin, L. X.; Ge, H. G.; Yu, X. H.; Wang, W. L. Significant enhancement in photovoltaic performances for C217-based dye sensitizers via introducing electron-withdrawing substituents: a theoretical study. *Chin. J. Struct. Chem.* **2019**, 38, 2041–2056.

(59) Zhang, L. S.; Jiang, X. H.; Zhong, Z. A.; Tian, L.; Sun, Q.; Cui, Y. T.; Lu, X.; Zou, J. P.; Luo, S. L. Carbon nitride supported high-loading iron single-atom catalyst for activating of peroxymonosulfate to generate oxygen with 100% selectivity. *Angew. Chem., Int. Ed.* **2021**, 60, 21751–21755.

(60) Sattler, W.; Henling, L. M.; Winkler, J. R.; Gray, H. B. Bespoke photoreductants: tungsten arylisocyanides. *J. Am. Chem. Soc.* **2015**, 137, 1198–1205.

(61) Sattler, W.; Ener, M. E.; Blakemore, J. D.; Rachford, A. A.; LaBeaume, P. J.; Thackeray, J. W.; Cameron, J. F.; Winkler, J. R.; Gray, H. B. Generation of powerful tungsten reductants by visible light excitation. *J. Am. Chem. Soc.* **2013**, 135, 10614–10617.

(62) Seki, T.; Tokodai, N.; Omagari, S.; Nakanishi, T.; Hasegawa, Y.; Iwasa, T.; Taketsugu, T.; Ito, H. Luminescent mechanochromic 9-anthryl gold(I) isocyanide complex with an emission maximum at 900 nm after mechanical stimulation. *J. Am. Chem. Soc.* **2017**, 139, 6514–6517.

(63) Smith, N. E.; Bernskoetter, W. H.; Hazari, N.; Mercado, B. Q. Synthesis and catalytic activity of PNP-supported iron complexes with ancillary isonitrile ligands. *Organometallics* **2017**, 36, 3995–4004.

(64) Suginome, M.; Nakamura, H.; Ito, Y. Optically active isonitrile ligand for palladium-catalyzed enantioselective bis-silylation of carbon-carbon double bonds. *Tetrahedron Lett.* **1997**, 38, 555–558.

(65) Gao, Q. D.; Yang, E. The first-principles study on the rectification of molecular junctions based on the alkyl-chain-modified [2,5']bipyrimidinyl-(biphenyl isocyanide)gold(I). *Chin. J. Struct. Chem.* **2020**, 39, 1763–1769.

(66) Johnson, K. N.; Hurlock, M. J.; Zhang, Q.; Hipps, K. W.; Mazur, U. Balancing noncovalent interactions in the self-assembly of nonplanar aromatic carboxylic acid MOF linkers at the solution/solid interface: HOPG vs. Au(111). *Langmuir.* **2019**, 35, 5271–5280.

(67) Leigh, W. J.; Arnold, D. R. Merostabilization in radical ions, triplets, and biradicals. 6. The excited state behavior of para-substituted tetraphenylethylenes. *Can. J. Chem.* **1981**, 59, 3061–3075.

DOI: 10.14102/j.cnki.0254-5861.2021-0049

(68) Lin, X. C.; Li, N.; Zhang, W. J.; Huang, Z. J.; Tang, Q.; Gong, C. B.; Fu, X. K. Synthesis and electrochromic properties of benzonitriles with various chemical structures. *Dyes Pigment.* **2019**, 171, 107783.
(69) Bhunia, A.; Vasylyeva, V.; Janiak, C. From a supramolecular tetranitrile to a porous covalent triazine-based framework with high gas uptake capacities. *Chem. Commun.* **2013**, 49, 3961–3963.
(70) Shustova, N. B.; McCarthy, B. D.; Dinca, M. Turn-on fluorescence in tetraphenylethylene-based metal-organic frameworks: an alternative to aggregation-induced emission. *J. Am. Chem. Soc.* **2011**, 133, 20126–20129.
(71) Shi, W.; Liu, Q.; Zhang, J.; Zhou, X. Y.; Yang, C.; Zhang, K. S.; Xie, Z. F. Tetraphenylethene-decorated functional polybenzoxazines: post-polymerization synthesis via benzoxazine-isocyanide chemistry and application in probing and catalyst fields. *Polym. Chem.* **2019**, 10, 1130–1139.
(72) Feng, H. T.; Yuan, Y. X.; Xiong, J. B.; Zheng, Y. S.; Tang, B. Z. Macrocycles and cages based on tetraphenylethylene with aggregation-induced emission effect. *Chem. Soc. Rev.* **2018**, 47, 7452–7476.
(73) Chen, Q.; Jia, C.; Zhang, Y.; Du, W.; Wang, Y.; Huang, Y.; Yang, Q.; Zhang, Q. A novel fluorophore based on the coupling of AIE and ESIPT mechanisms and its application in biothiol imaging. *J. Mater. Chem. B.* **2017**, 5, 7736–7742.
(74) Chen, P. F.; Zhu, H. C.; Kong, L.; Xu, X. Y.; Tian, Y. P.; Yang, J. X. Multifunctional behavior of a novel tetraphenylethylene derivative: mechanochromic luminescence, detection of fluoride ions and trace water in aprotic solvents. *Dyes Pigment.* **2020**, 172, 107832.
(75) Li, Q.; Niu, Z. G.; Liu, Y. L.; Wang, E. J. Crystal structure and aggregation-induced emission of an azine derivative. *Chin. J. Struct. Chem.* **2020**, 39, 693–697
(76) Gorvin, J. H. Polyphenylethylenes. Part I. Preparation and characteristics of tetrakis(p-nitrophenyl)ethylene. *J. Chem. Soc.* **1959**, 678–682.
(77) Xu, S. Y.; Bai, X. L.; Ma, J. W.; Xu, M. M.; Hu, G. F.; James, T. D.; Wang, L. Y. Ultrasmall organic nanoparticles with aggregation-induced emission and enhanced quantum yield for fluorescence cell imaging. *Anal. Chem.* **2016**, 88, 7853–7857.

Received: December 25, 2021
Accepted: April 7, 2022
Published: April 8, 2022

DOI: 10.14102/j.cnki.0254-5861.2021-0049